Journal of Numerical Analysis and Applied Mathematics
Vol. 2, No. 2, 2017, pp. 6-14
http://www.aiscience.org/journal/jnaam

Numerical Solutions of Double-Diffusive Natural Convection Flow of MHD Casson Fluid over a Stretching Vertical Surface with Thermal Radiation

K. Ganesh Kumar[1], G. K. Ramesh[2, *], B. J. Gireesha[1]

[1]Department of Studies and Research in Mathematics, Kuvempu University, Shimoga, Karnataka, India
[2]Department of Mathematics, School of Engineering, Presidency University, Bengaluru, Karnataka, India

Abstract

This investigation deals with an influence of thermal radiation effect on a double-diffusive convection flow of MHD Casson fluid over a stretching vertical surface. The governing partial differential equations are remodeled into ordinary differential equations by using similarity transformation. The ensuing differential equations are resolved numerically by using Runge-Kutta-Fehlberg forth-fifth technique (RKF45 Method). The results of flow and heat analysis on velocity and temperature profiles are given diagrammatically. The numerical values of the local skin friction coefficient, local Nusselt number and local Sherwood number also are shown in a tabular form. Results shows that Casson parameter enhance the velocity and suppress the temperature, concentration fields but opposite effect can be found the presence of Buoyancy force.

Keywords

Casson Fluid, Double-Diffusive Convection, Thermal Radiation, Magnetic Field, Vertical Surface

Received: July 23, 2017 / Accepted: August 8, 2017 / Published online: September 18, 2017

1. Introduction

The phenomenon of radiative heat transfer is important with regard to tremendous applications like electrical power generation, solar system technology, space vehicles, missiles, propulsion devices for aircraft, nuclear plants, astrophysical flows, and many others. Although ample studies were generated for the boundary layer flow in the presence of thermal radiation, the fluid thermal conductivity in such cases is treated as a constant. This perhaps is not realistic because it is now proven that the thermal conductivity of liquid metals varies linearly with temperature from 0◦F to 400◦F [1]. Thus, the effects of viscous dissipation and thermal radiation in the flow of a viscous fluid over a permeable stretching sheet were analyzed by Cortell [2]. Ramesh et al. [3] discussed the effects of magnetic field and thermal radiation on Maxwell fluid over a stretching sheet in the presence of nanoparticles. Hayat and Qasim [4] examined the influence of thermal radiation and Joule heating on MHD flow of a Maxwell fluid in the presence of thermophoresis. Makanda et al [5] who studied the effects of radiation on MHD free convection of a Casson fluid from a horizontal circular cylinder with partial slip in non-Darcy porous medium with viscous dissipation. Typical works can be found in [6-9].

Researchers are paying their attention to investigate the double diffusive mixed convection flow because of their numerous technological applications, such as chemical engineering, solid-state physics, oceanography, geophysics, liquid gas storage, production of pure medication, oceanography, high-quality crystal production, solidification

* Corresponding author
E-mail address: gkrmaths@gmail.com (G. K. Ramesh)

of molten alloys and exothermally heated lakes and magmas etc. Gaikwad et al [10] discussed the linear and non-linear double diffusive convection with Soret and Dufour effects in couple stress fluid. Soret and Dufour effect on double diffusion mixed convection from a vertical surface in a porous medium saturated with a non-Newtonian fluid has been carried out by Mahdy [11]. Khan and Aziz [12] analyzed the double-diffusive natural convective boundary layer flow in a porous medium saturated with ananofluid over a vertical plate by considering prescribed surface heat, solutal and nanoparticle fluxes. Nield and Kuznetsov [13] presented the double-diffusive nanofluid convection in a porous medium using analytical method. Abidi et al [14] carried out the effect of radiative heat transfer on three-dimensional double diffusive natural convection. Subhashini et al [15]. Beg et al [16], Goyal and Bhargava [17] are some of the works associated with stretching sheet problem of double diffusive mixed convection.

The diversity of nature flow develops the various rheological properties of liquids. The different industrial processes like plastic material production, paints production, preventative coating, lubricants performance and many others involve the rheological liquids of various characteristics. All the rheological aspects of liquids cannot be described by simple theory of Navier-Stokes. For the exact description of rheological liquids, different fluid models like power-law models, Powell-Eyring liquid, Jeffrey, Maxwell and Oldroyd-B fluids, Casson fluid etc. have been formulated according to physical characteristics of non-Newtonian materials. The present research dealt with Casson liquid model which is proposed by suspension of cylindrical shaped particles in liquid. Few common examples of Casson liquid include blood, waxy crude oils, gum solutions, slurries etc. This model is appropriate to explore the mechanism of pseudo plastic yield stress liquids. The model is firstly reported by Wilkinson [18]. The various dimensions and aspects of Casson liquid have beenexplored by Walwander et al. [19] and Joy [20]. Hayat et al. [21] presented the analysis of Casson liquid flow under the effects of Dufour and Soret. In another study, Hayat et al. [22] considered the coupled flow of Casson liquid with mixed boundary condition. Bhattacharyya [23] elaborated stagnation point Casson fluid flow with heat transport. Impact of entropy generation in Cassonnanoliquid flow due to moving surface has been addressed by Abolbashari et al. [24]. Maity et al. [25] discussed three-dimensional time-dependent flow of Casson liquid with injection/suction. Abbas et al. [26] computed numerical solutions to discuss the chemically reactive flow of Casson fluid with solar radiation. Some recent contributions through Casson fluid for different geometry can be seen in [27-29]

The main objective of the present investigation is to study the effect of thermal radiation on double-diffusive natural convection flow of Casson fluid past a stretching vertical surface with magnetic field. The method of solution involves similarity transformation which reduces the partial differential equations into a set of non-linear ordinary differential equations. These non-linear ordinary differential equations have been solved by applying Runge-Kutta-Fehlberg forth-fifth order method (RKF45 Method) with help of shooting technique. The velocity and temperature profiles for different values of flow parameters are presented in the figures. It is observed from all figures that the boundary conditions are satisfied asymptotically in all the cases which support the accuracy of numerical results.

2. Formulation of the Problem

A steady two dimensional laminar mixed convection flow over a stretching vertical surface in a viscous fluid of temperature T_∞ and concentration C_∞ (see Fig. 1) is considered. The stretching velocity is assumed to be of the form $u_w(x) = b\sqrt{x}$ where b is constant with $b > 0$, T_w and C_w are temperature and concentration at the wall assumed to be constant. The buoyancy forces arise due to the variations in temperature and concentration of fluid. The Boussinesq approximation is invoked for the fluid properties to relate the density changes to temperature and concentration and to couple in this way the temperature and concentration fields to the flow field. Under these assumptions, the governing boundary layer equations can be expressed as

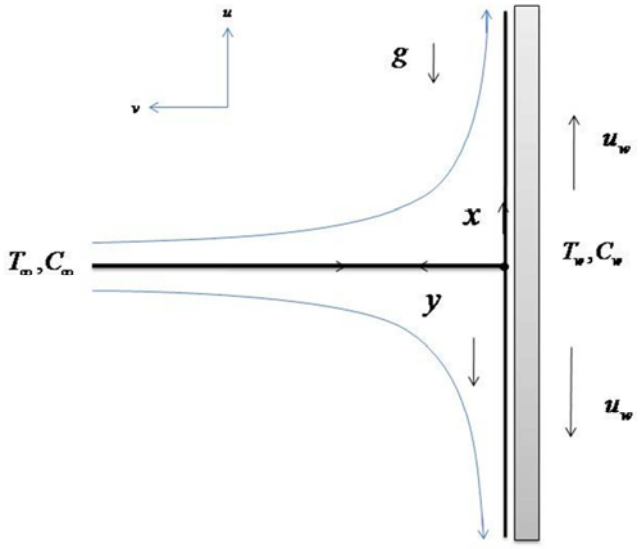

Figure 1. Schematic diagram of the problem.

$$\frac{\partial u}{\partial x} + \frac{\partial v}{\partial y} = 0, \tag{1}$$

$$u\frac{\partial u}{\partial x}+v\frac{\partial u}{\partial y}=\upsilon(1+\frac{1}{\beta})\frac{\partial^2 u}{\partial y^2}+g\beta^*(T-T_\infty)+g\beta^{**}(C-C_\infty)-\frac{\sigma B_0^2}{\rho}u, \quad (2)$$

$$u\frac{\partial T}{\partial x}+v\frac{\partial T}{\partial y}=\alpha\frac{\partial^2 T}{\partial y^2}-\frac{\partial q_r}{\partial y}, \quad (3)$$

$$u\frac{\partial C}{\partial x}+v\frac{\partial C}{\partial y}=D\frac{\partial^2 C}{\partial y^2}, \quad (4)$$

with the relevant boundary conditions

$$u=u_w,\ \ v=0,\ \ T=T_w,\ \ C=C_w \text{ at } y=0,$$

$$u=0,\ \ T\to T_\infty,\ \ C\to C_\infty \text{ at } y\to\infty. \quad (5)$$

Using the Rosseland approximation for radiation, radiation heat flux q_r is simplified as,

$$q_r=-\frac{4\sigma^*\partial T^4}{3k^*\partial y}=-\frac{16\sigma^*}{3k^*}T_\infty^3\frac{\partial T}{\partial y}, \quad (6)$$

where σ^* and k^* are the Stefan – Boltzmann constant and the mean absorption coefficient respectively.

In view to Eq. (6), Eq. (3) reduces to

$$u\frac{\partial T}{\partial x}+v\frac{\partial T}{\partial y}=\frac{\partial}{\partial y}\left[\alpha\left(1+\frac{16\sigma^*T_\infty^3}{3k^*k}\right)\frac{\partial T}{\partial y}\right], \quad (7)$$

the following similarity transformations are introduced to Eqs. (1)–(4),

$$\varphi=(\upsilon x u_w(x))^{\frac{1}{2}}f(\eta),$$

$$\theta(\eta)=\frac{T-T_\infty}{T_w-T_\infty},\ \ \phi(\eta)=\frac{C-C_\infty}{C_w-C_\infty},\ \ \ \eta=\left(\frac{u_w(x)}{\upsilon x}\right), \quad (8)$$

where φ is the stream function defined in the usual form as,

$$u=\frac{\partial\phi}{\partial y} \text{ and } v=-\frac{\partial\phi}{\partial x}.$$

Eq. (1) is identically satisfied and the velocity components u and v are given by

$$u=u_w(x)f'(\eta),\ \ \ v=-\frac{1}{4}\left(\frac{u_w(x)}{\upsilon x}\right)(3f-\eta f'), \quad (9)$$

where prime denotes differentiation with respect to η. Therefore, substituting the new variables (8) and (9), Eqs. (2)–(4) are reduced to the following set of ordinary differential Eqs.,

$$\left(1+\frac{1}{\beta}\right)f'''+\frac{3}{4}f''f-\frac{1}{2}f'^2+\lambda(\theta+N\varphi)-Mf'=0, \quad (10)$$

$$\left(1+\frac{4}{3}R\right)\theta''+\Pr\frac{3}{4}\theta' f=0, \quad (11)$$

$$\varphi''+Sc\frac{3}{4}\varphi' f=0, \quad (12)$$

Along the transformed boundary conditions (5) are

$$f'(\eta)=1,\ f(\eta)=0\ \theta(\eta)=1,\ \phi(\eta)=1 \text{ at } \eta=0,$$

$$f'(\eta)=0,\ \ \theta(\eta)=0,\ \varphi(\eta)=0 \text{ as } \eta\to\infty, \quad (13)$$

where η_∞ is the edge of the boundary layer. Here $\lambda=\lambda_1(x)$ is the mixed convection parameter and $N=N(x)$ is the buoyancy force parameter, which are given by

$$\lambda_1(x)=Gr_x,\ \ N(x)=\frac{Gr^*}{Gr},$$

With $Gr=\frac{g\beta^*(T_w-T_\infty)}{b^2}$ and $Gr^*=\frac{g\beta^{**}(C_w-C_\infty)}{b^2}$ are the Grashof numbers and $Re_x=\frac{u_w(x)x}{\upsilon}$ is the local Reynolds number, $M=\frac{\sigma B_0^2 u_w}{\rho b^2}$ is the magnetic parameter, $\Pr=\frac{\upsilon}{\alpha}$ is the Prandtl number, $Sc=\frac{\upsilon}{D}$ is the Schmidt number, $R=\frac{4\sigma^*T_\infty^3}{k^*k}$ is the radiation parameter. On the other hand, it should be noticed that because $\lambda=\lambda_1(x)$ and $N=N(x)$,Eqs. (8)–(10) are only locally similarity equations. λ_1 and N will be further considered as constants. It may be noted that $\lambda_1>0$ corresponds to assisting flow (the external velocity is opposite to the acceleration due to gravity), $\lambda_1<0$ corresponds to opposing flow (the external velocity and the acceleration due to gravity have the same direction) and $\lambda_1=0$ corresponds to force convection flow (non-buoyant case).

The physical quantities of interest are the skin friction coefficient C_f , local Nusselt number Nu_x and the Sherwood number Sh_x as defined by,

$$C_f=\mu\left(\frac{\partial u}{\partial y}\right)_{y=0},\ \ \ q_w=-k\left(\frac{\partial T}{\partial y}+q_r\right)_{y=0} \text{ and } j_w=-D_m\left(\frac{\partial C}{\partial y}\right)_{y=0}.$$

Using similarity transformations and we get;

$$C_f(Re_x)^{\frac{1}{2}}=\left(1+\frac{1}{\beta}\right)f''(0),\ \ Nu_x(Re_x)^{-\frac{1}{2}}=\left[1+\frac{4}{3}R\right]\theta'(0) \text{ and}$$

$$Sh_x (Re_x)^{\frac{1}{2}} = -\varphi'(0).$$

3. Results and Discussion

The system of coupled extremely non-linear ordinary differential equations (10)–(12) subject to the boundary conditions (13) is resolved numerically using Runge-Kutta-Feldberg 45 technique. This method has been successfully used by the present authors to resolve numerous problems associated with boundary layer flow and heat and mass transfer. During this method, the end of the boundary layer η_∞ has been chosen as $\eta = 6$ that is sufficient to realize the far field boundary conditions attention for all values of the parameters considered. Comprehensive numerical parametric computations are carried out for various physical parameters values then the results are reported in terms of graphs. Numerical solutions obtained for the problem are expressed in terms of graphs for various ranges and for various choices of the flow parameters. Impact of magnetic parameter, radiation parameter, Schmidt number, Prandtl number, mixed convection parameter, buoyancy parameter, non-Newtonian Casson parameter on rate, temperature and concentration profiles are mentioned.

Figure 2-4 illustrates the variations of velocity, temperature and concentration profiles for numerous values of Cassonparameter (β). From figure 2, we tend to determined that the velocity profile decreases once an increasing β. An uplifting the values of β, leads to an increase in dynamic viscosity that produces resistance within the flow of fluid and a decrease in fluid velocity is determined. Figure 3 and 4 presents that the larger values of Casson parameter produce an improvement within the temperature profile, concentration profile and associated boundary layer thickness.

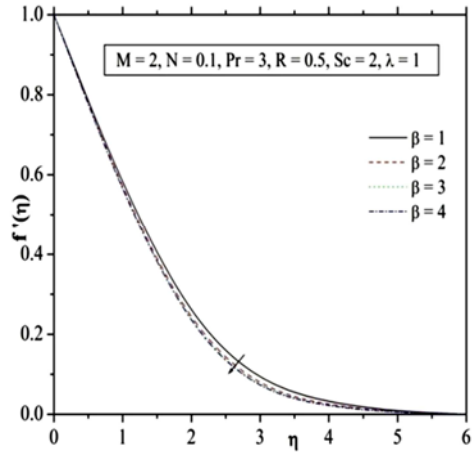

Figure 2. Velocity profile for various values of Casson parameter.

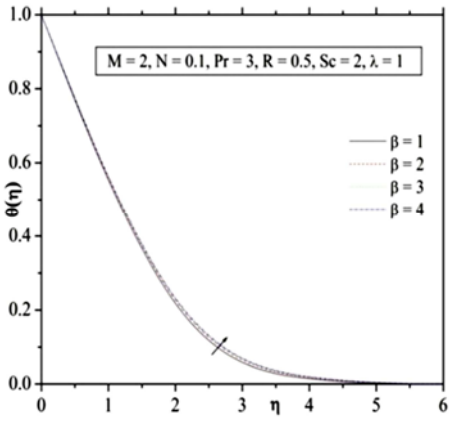

Figure 3. Temperature profile for various values of Casson parameter.

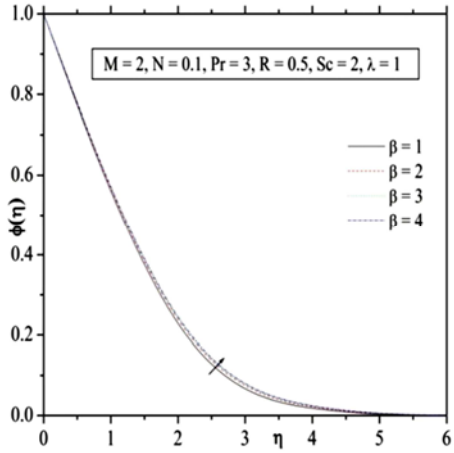

Figure 4. Concentration profile for various values of Casson parameter.

Figure 5-7 displays the impact of mixed convection parameter (λ) on velocity, temperature and concentration profiles severally. Velocity profile and boundary layer thickness increase for the higher values of mixed convection parameter λ as shown in figure 5. In figure 6 and 7, it's determined that the increase in λ causes a reduction in temperature, concentration profiles and additionally as thermal boundary layer thickness.

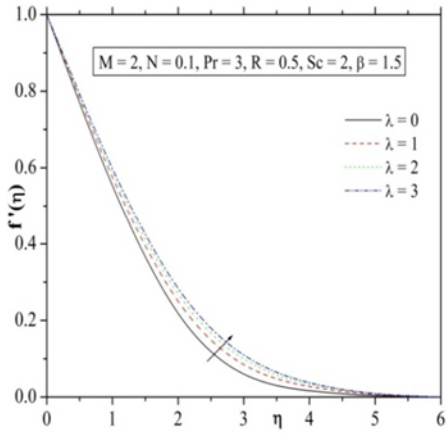

Figure 5. Velocity profile for various values of mixed convection parameter.

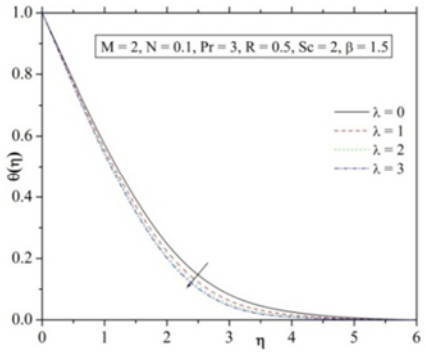

Figure 6. Temperature profile for various values of mixed convection parameter.

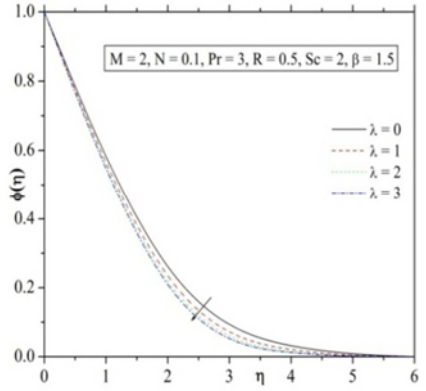

Figure 7. Concentration profile for various values of mixed convection parameter.

The developments of the magnetic parameter (M) on velocity temperature and concentration profiles are shown in Figure 8-10 respectively. In figure 8, it's determined that the velocity profile decreases with the rise of the magnetic parameter values, as a results of the presence of a magnetic field in an electrically conducting fluid introduces a force referred to as the Lorentz force, that acts against the flow if the magnetic field is applied in the normal direction, as within the gift study. This resistive force slows down the fluid velocity. For both the temperature and concentration profiles will increase by increasing the values of magnetic parameter component as shown in figure 9 and 10.

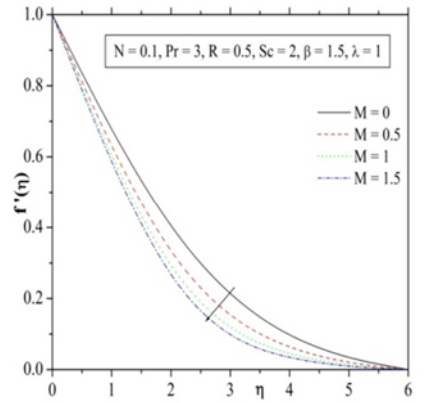

Figure 8. Velocity profile for various values of magnetic parameter.

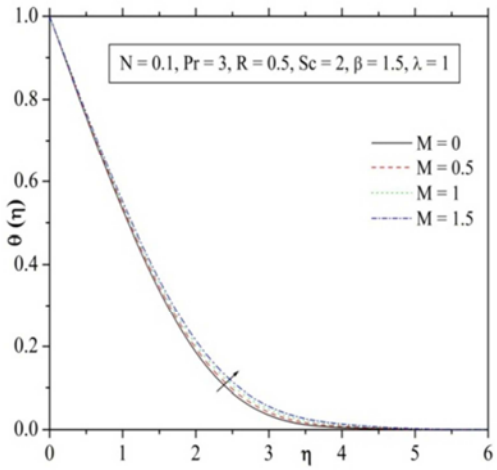

Figure 9. Temperature profile for various values of magnetic parameter.

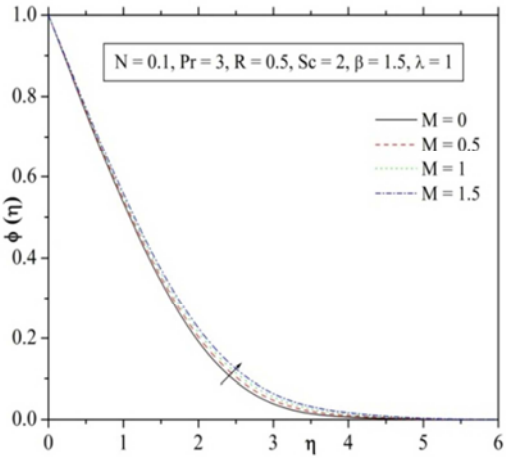

Figure 10. Concentration profile for various values of magnetic parameter.

The impact of buoyancy parameter (N) for velocity, temperature and concentration profiles is illustrated in Figure 11-13. Here both the velocity and boundary layer thickness increase for increasing N. But in the case of temperature and concentration profiles raises the buoyancy parameter its exhibits opposite behaviour of the velocity profile.

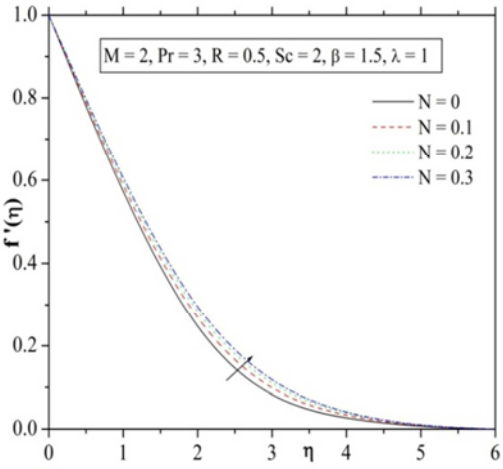

Figure 11. Velocity profile for various values of buoyancy force parameter.

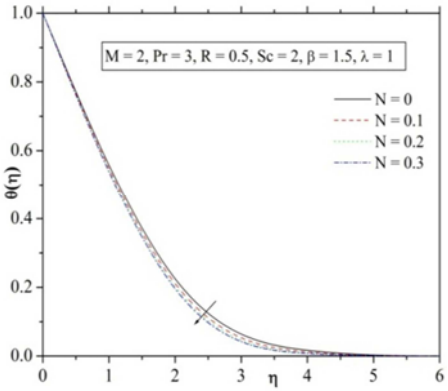

Figure 12. Temperature profile for various values of buoyancy force parameter.

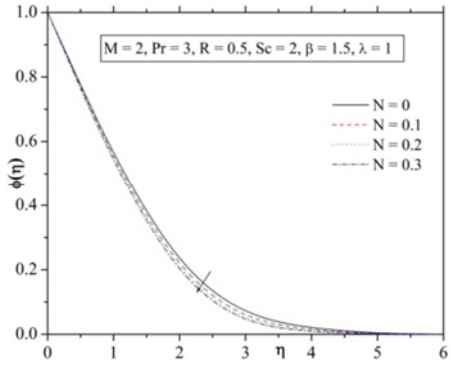

Figure 13. Concentration profile for various values of buoyancy force parameter.

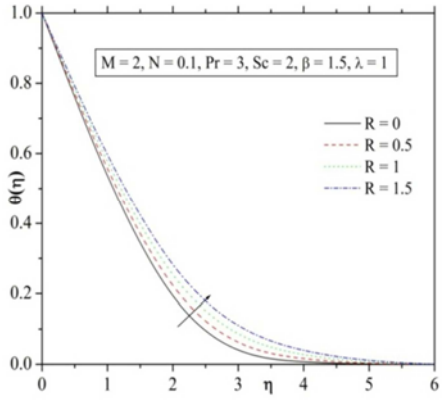

Figure 14. Temperature profiles for various values of R .

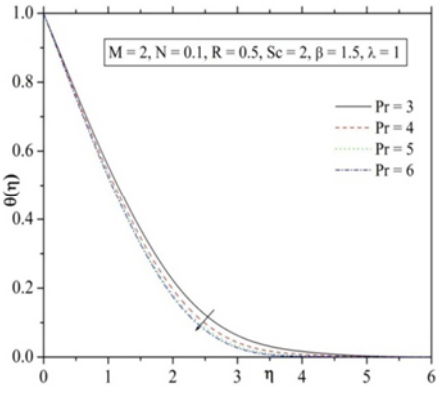

Figure 15. Temperature profiles for various values of Pr .

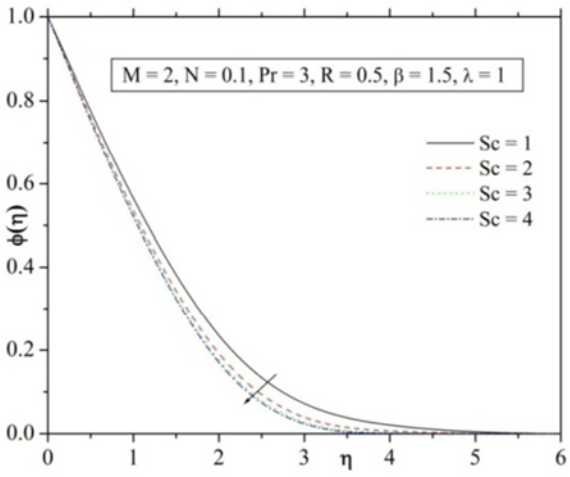

Figure 16. Concentration profile for various values of Schmidt number.

The result of radiation parameter (R) on the temperature profile is given in figure 14. From this figure we tend to observe that, as the value of R increases the temperature profiles will increase, additionally an increasing in the thermal boundary layer thickness. Figure 15 shows the variation of the temperature profile for numerous values of Prandtlnumber (Pr). The result shows that an increases of Prandtl number leads to a decreasing the thermal boundary layer thickness. The reason is that smaller values of Pr are similar to increasing the thermal conductivities, and so, heat is ready to differ far away from the heated surface quicker than for higher values of Pr. Hence, the boundary layer is thicker and also the rate of heat transfer is reduced, for gradient are reduced. Figure 16 shows the concentration profiles across the physical phenomenon for numerous values of Schmidt number (Sc) The figure shows that an increasing in Sc leads to a decreasing the concentration distributions, as a results of the smaller values of Sc are reminiscent of increasing the chemical molecular diffusivity.

Fig 17 shows the relation between mixed convection parameter and Casson parameter, which is proportional to skin friction coefficient. This figure depicts that the skin friction coefficient decreases with an increasing λ and β parameter. The local skin friction coefficient increases by increasing β and M as show in figure 18. Figure 19 and 20 shows the impact of λ and Pr with the various value of R respectively for Nusselt number. The local Nusselt number is an increasing behaviour for higher values of the mixed convection parameter versus radiation parameter and the Prandtl number versus radiation parameter. Figure 21 illustrates the variations in the mixed convection parameter and Schmidt number on Sherwood number. From this figure it's clear that an increase λ and Sc will increase the Sherwood number.

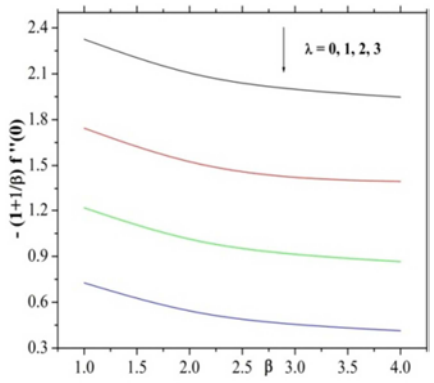

Figure 17. Skin friction coefficient for several values of λ verses β.

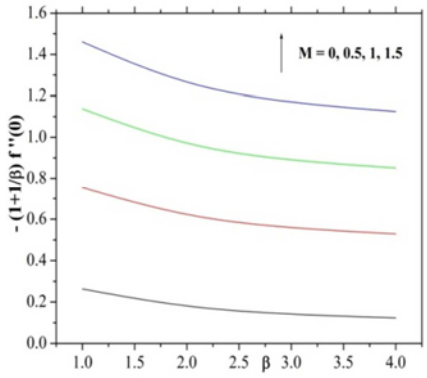

Figure 18. Skin friction coefficient for several values of M verses β.

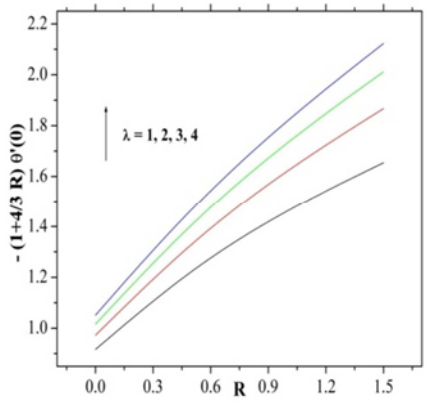

Figure 19. Nusselt number for several values of λ verses R.

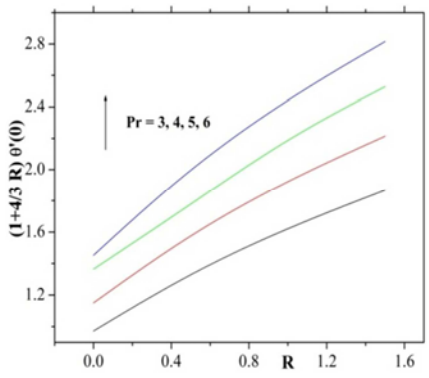

Figure 20. Nusselt number for several values of Pr verses R.

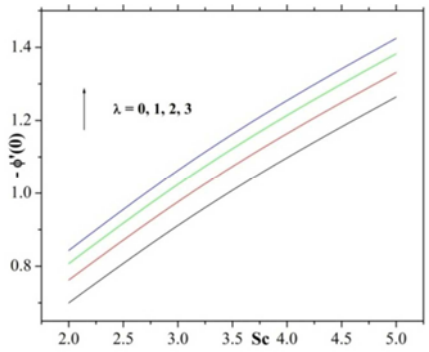

Figure 21. Sherwood number for several values of the λ with Sc.

4. Conclusion

Influence of thermal radiation on double-diffusive convection MHD Casson fluid over a stretching vertical surface in the presence of magnetic field is presented. Numerical results for velocity profiles, surface heat transfer rate and mass transfer rate are obtained for constant variations of varied ranges and for the various values of flow pertinent parameters. The most outcomes of the problem are summarized as follows;

a. Magnetic field and Casson parameter increase the velocity profile whereas reducing the temperature and concentration profiles;

b. Buoyancy force due to temperature difference reduces the skin friction whereas will increase the local Nusselt and Sherwood numbers;

c. Increasing the mixed convection parameter will increase velocity, local Nusselt number and local Sherwood number and decreases the skin friction coefficient, temperature and concentration profiles.

d. Higher Schmidt number caused the numerous reductions in concentration boundary layer thickness.

e. Thermal boundary layer thickness increase by increasing the radiation parameter but within the case of Prandtl number it exhibit opposite behaviour of radiation parameter.

Nomenclature

B_0	magnetic field strength
C	fluid concentration
C_f	local skin friction coefficient
D	mass diffusivity
f	dimensionless stream function
g	dimensionless velocity

Gr_x, Gr_x^*	local Grashof numbers
k	thermal conductivity
N	ratio of buoyancy parameters
Nu_x	Local Nusselt number
M	Magnetic parameter
Pr	Prandtl number,
Re_x	local Reynolds number based on x
R	radiation parameter
Sc	Schmidt number,
Sh_x	local Sherwood number
T	fluid temperature in the boundary layer
u, v	velocity components in the - x and y - directions, respectively
$u_w(x)$	velocity of the stretching surface
x, y	Cartesian coordinates

Greek Symbols

α	thermal diffusivity
β	Casson parameter
β^*	volumetric coefficient of thermal expansion
β^{**}	volumetric coefficient of expansion for concentration
η	similarity variable
θ	dimensionless temperature variable
λ	buoyancy parameter
μ	dynamic viscosity
υ	kinematic viscosity
ϕ	dimensionless concentration
φ	dimensional stream function

Subscripts

∞	infinity
w	sheet surface

References

[1] WMKay, *Convective Heat and Mass Transfer*, McGraw-Hill, New York, 1966.

[2] R Cortell, Combined effects of viscous dissipation and thermal radiation on fluid flows over a non-linearly stretched permeable wall. *Meccanica*, 2012, 477, 769–81.

[3] GK Ramesh, BJ Gireesha, T Hayat, and A Alsaedi, Stagnation point flow of Maxwell fluid towards a permeable surface in the presence of nanoparticles, *Alexandria Engineering Journal,* 2016, 53, 857-65.

[4] T Hayat and M Qasim, Influence of thermal radiation and Joule heating on MHD flow of a Maxwell fluid in the presence of thermophoresis, *Int. J. Heat and Mass Transfer*, 2010, 53, 4780–88.

[5] G Makanda, S Shaw and P Sibanda, Effects of radiation on MHD free convection of a Casson fluid from a horizontal circular cylinder with partial slip in non-Darcy porous medium with viscous dissipation, *Boundary Value Problems* 2015, 2015, 75, 1-14.

[6] GK Ramesh and BJ Gireesha, Flow over a stretching sheet in a dusty fluid with radiation effect, *ASME J. Heat transfer*, 2013,135(10), 102702(1-6).

[7] P Bala and A Reddy, Magnetohydrodynamic flow of a Casson fluid over an exponentially inclined permeable stretching surface with thermal radiation and chemical reaction, *Ain Shams Engineering Journal*, 2016, 7(2), 593–602.

[8] GK Ramesh, BJ Gireesha andCS Bagewadi, Stagnation point flow of a MHD dusty fluid towards a stretching sheet with radiation, Afrika Matematika,2014, 25 (1), 237-249.

[9] L Zheng, C Zhang, X Zhang and J Zhang, Flow and radiation heat transfer of a nanofluid over a stretching sheet with velocity slip and temperature jump in porous medium, *Journal of the Franklin Institute*, 2013, 350(5), 990–1007.

[10] SNGaikwad, MSMalashetty and KR Prasad, An analytical study of linear and non-linear double diffusive convection with Soret and Dufour effects in couple stress fluid, *Int. J. Non-Linear Mech*., 2007, 42, 903–13.

[11] AMahdy, Soret and Dufour effect on double diffusion mixed convection from vertical surface in a porous medium saturated with a non-Newtonian fluid, *J. Non-Newton. Fluid Mech*., 2010, 165, 568–75.

[12] WA Khan and A Aziz, Double-diffusive natural convective boundary layer flow in porous medium saturated with a nanofluid over a vertical plate: prescribed surface heat, solutal and nanoparticle fluxes, *Int. J. Therm. Sci*., 2011, 726, 2154–160.

[13] AV Kuznetsov and DA Nield, The Cheng–Minkowycz problem for the double-diffusive naturalconvective boundary layer flow in a porous medium saturated by a nanofluid, *Int. J. Heat and Mass Transfer*, 2011, 54, 374–78.

[14] A Abidi, LKolsi, MN Borjini and HBAissia, Effect of radiative heat transfer on three-dimensional double diffusive natural convection, *Numerical Heat Transfer, Part A: applications: An Int. J. Computation and Methodology*, 2011, 60(9), 785-809.

[15] SV Subhashini, RSumathi and I Pop, Dual solutions in a double-diffusive MHD mixed convection flow adjacent to a vertical plate with prescribed surface temperature, *Int. J. Heat and Mass Transfer*, 2013, 56, 724-731.

[16] OA Beg, MJUddin, MM Rashidi and NKavyani, Double-diffusive radiative magnetic mixed convective slip flow with Biot and Richardson number effects, *J. Eng. Therm. phys*., (2014) 23(2), 79–97.

[17] M Goyal and RBhargava, Finite element solution of double diffusive boundary layer flow of viscoelastic nanofluids over a stretching sheet, *Comput. Math. and Mathematical Phys*., 2014, 54(5), 848–63.

[18] WL Wilkinson, *Non-Newtonian fluids*, Pergamon, NewYork, 1960.

[19] WP Walwander, TY Chen and DF Cala, An approximate Casson fluid model for tube flow of blood, *Bio-Rheology,* 1975,12, 111-19.

[20] DDJoye, Shear rate and viscosity corrections for a Casson fluid in cylindrical (Couette) geometries, *Journal of Colloid and Interface Science,* 2003, 267, 204-10.

[21] T Hayat, SA Shehzad and A Alsaedi, Soret and Dufour effects on magnetohydrodynamic (MHD) flow of Casson fluid, *Applied Mathematics and Mechanics*, 2012, 33, 1301-12.

[22] T Hayat, SAShehzad, A Alsaedi and MSAlhothuali, Mixed convection stagnation point flow of Casson fluid with convective boundary conditions, *Chinese Physics Letters*, 2012, 29, 114704.

[23] KBhattacharyya, MHD stagnation-point flow of Casson fluid and heat transfer over a stretching sheet with thermal radiation, *Journal of Thermodynamics*, 2013, 2013, 169674.

[24] MH Abolbashari, NFreidoonimehr, F Nazari and MMRashidi, Analytical modeling of entropy generation for Cassonnano-fluid flow induced by a stretching surface, *Advanced Powder Technology*, 2015, 26, 542-52.

[25] S Maity, SK Singh and AV Kumar, Unsteady three dimensional flow of Casson liquid film overa porous stretching sheet in the presence of uniform transverse magnetic field and suction/injection, *Journal of Magnetism and Magnetic Materials,*2016, 419, 292-300.

[26] Z Abbas, M Sheikh and SS Motsa, Numerical solution of binary chemical reaction on stagnation point flow of Casson fluid over a stretching/shrinking sheet with thermal radiation, *Energy*, 2016, 95, 12-20.

[27] R UlHaq, S Nadeem, ZH Khan and TG Okedayo, Convective heat transfer and MHD effects on Cassonnanofluid flow over a shrinking sheet, *Cent. Eur. J. Phys*., 2014, 12(12), 862-71.

[28] GK Ramesh, BC Prasanna Kumara, BJ Gireesha and MM Rashidi, Casson fluid flow near the stagnation point over a stretching sheet with variable thickness and radiation, *Journal of Applied Fluid Mechanics*, 2016, 9(3),1115-22.